

HYDROELASTIC EFFECTS OF A LOSS OF COOLANT IN A PRESSURIZED WATER REACTOR

J. K. DIENES, C. W. HIRT, W. C. RIVARD, L. R. STEIN, M. D. TORREY

*Theoretical Division, Group T-3, University of California, Los Alamos Scientific Laboratory,
P.O. Box 1663, Los Alamos, New Mexico 87545, U.S.A.*

SUMMARY

With the increasing demand for precise statements of nuclear reactor safety margins, and the importance of achieving the most efficient possible designs, there has emerged a need to develop more detailed analyses for reactor safety. In pressurized water reactors the design of the Core Support Barrel (CSB) is strongly influenced by the possibility of a cold leg break, which would lead to a large transient pressure differential across the CSB. In a first analysis it is natural to estimate its response as a cantilever beam, but because the shell is quite thin, and the length of the CSB rarely exceeds twice its radius, the possibility that local deformations might be important needs to be considered. For that reason we have written a series of combined shell-fluid computer codes to analyze the dynamic interactions. In SOLA-FLX1 only axial motion of the fluid is allowed, and in SOLA-FLX2 circumferential motion is added. In K-FIX(3D,FLX) radial motion of the fluid is allowed as well, and this permits three-dimensional motion of fluid in the core.

We have found that the influence of the fluid in the downcomer region is greater than originally expected because of its large virtual mass, and that the influence of the fluid in the core is relatively small, and can be largely accounted for by treating it as a single element. Validation of these results and of the code will be obtained by detailed comparisons with data obtained in the large-scale HDR tests to be conducted by the Kernforschungszentrum Karlsruhe.

One curious phenomenon is that the initial deflection of the bottom of the CSB is away from the broken pipe rather than towards it. This effect can be explained by the formation of a local outward bulge in the shell that travels downward, forcing fluid ahead of it with a resulting increase in pressure, which in turn forces the shell inward.

Comparisons of computed strain histories with measurements in small scale axisymmetric tests show agreement of the peak strains on the order of 30% when the pressure release is represented by a sudden drop. However, the timing of the peaks is not good unless details of the pressure release mechanism, a double-diaphragm, are accounted for. When this is done, quite good agreement is obtained.

1. Introduction

The response of the internals of a pressurized water reactor (PWR) to a sudden loss of coolant can be investigated in a number of ways, as indicated by the wide variety of approaches discussed at the 4th International Conference on Structural Mechanics in Reactor Technology in 1977 [1-11]. The loss of fluid, in particular, can be analyzed by Eulerian methods, Lagrangian methods with rezone, finite element methods or, in fluid regions not affected by flashing or strong convection, simply by an acoustic approximation. The structural elements can be approximated by beam elements, modeled by finite element methods, represented by modal superposition or described by finite-difference approximations to the shell equations. The ultimate test of these methods will be how the results compare with experiments, though speed, flexibility and generality are important considerations. In our developmental work at LASL we have tended to emphasize finite-difference methods, both in the fluid and structural aspects of the problems. A summary of the method is given by Dienes, Hirt and Stein [12].

In this paper we will be summarizing recent results in two areas. In the first, we compare the results of axisymmetric calculations and experiments. This is followed by a comparison of two and three dimensional calculations using SOLA-FLX for the former and K-FIX (3D-FLX) for the latter.

2. Comparison of Axisymmetric Calculations and Experiments

The complexity of the complete loss-of-coolant hydroelastic problems in PWR safety analysis is so great that it appeared judicious to verify the computational methods in some simple geometries before proceeding to a full three-dimensional calculation. Not only does this make it possible to examine many details of the processes in a simple configuration, but it provides test problems for checking the more complex two- and three-dimensional codes. The axisymmetric geometry for such a series of calculations and experiments is illustrated in Fig. 1. The dimensions are essentially those of a 1/25 scale PWR, except for the axial arrangement of the pressure release pipe. The system is designed to have interchangeable cylinders. A thick cylinder, which approximates a rigid cylinder, is shown on the left. This arrangement is intended to examine the pressure drop in the absence of structural deformation. On the right is shown a cylinder whose thickness is scaled from that of a PWR.

The equation of motion of an elastic cylinder undergoing radial motion, w , is given by Timoshenko [13] as

$$\rho h \ddot{w} + D w'''' + E h w / a^2 = p$$

where ρ denotes the shell density; h , the thickness; a , the radius; E , Young's modulus and

$$D = E h^3 / 12(1 - \nu^2)$$

with ν for Poisson's ratio. The appropriate boundary conditions are

$$w(0, t) = \dot{w}(0, t) = 0$$

describing a damped condition at the top, and

$$w''(\ell, t) = w'''(\ell, t) = 0$$

for the free condition at the bottom, with ℓ the length of the shell. The equations are differenced in a straightforward way in SOLA-FLX, except that a special treatment of the boundary conditions is necessary to get good accuracy, as discussed in Ref. 12. The motion of the fluid is calculated using the SOLA-DF code, which is described in Ref. 14. A simple test problem for the coupled code concerns the situation in which the exit velocity of the fluid adjacent to the top of the CSB is prescribed. In that case a coupled wave travels downward at a theoretical velocity of

$$c^* = c_0 / (1 + \rho_0 c_0^2 a^2 / Ehb_0)^{1/2}$$

where c_0 denotes the speed of sound in the fluid, 1.06×10^5 cm/s, ρ_0 denotes its density, 0.74 g/cm³, and b_0 is the width of the downcomer, 0.84 cm. This equation may be readily obtained by considering the conservation of mass and momentum across a discontinuity in pressure, in combination with the linearized equation of state

$$p - p_0 = c_0^2 (\rho - \rho_0)$$

The same analysis leads to the pressure drop

$$\Delta p = \rho_0 c^* u = 31 \times 10^6 \text{ d/cm}^2$$

for an exit velocity of 628 cm/sec. The result of a numerical calculation with SOLA-FLX is shown in Fig. 2. Though it exhibits considerable structure that is not forthcoming from the jump conditions, the mean velocity of the wave is consistent with the 64% reduction predicted by this analysis, and the pressure drop is very near the 31 bars obtained above.

Experiments were carried out at Systems, Science and Software (S³) to test the computer simulation. In the first series of experiments a linear shaped charge was used to cut the piping. Unfortunately, this device caused an initial shock to propagate into the system, and its reverberations obscured the depressurization process. As a result, a new study was undertaken to establish the improvement resulting from a double diaphragm pressure release system, illustrated in Fig. 3. The pressure differential across the lower diaphragm is maintained at $p_0/2$ by a hydraulic device during pressurization. When p_0 has reached the desired value, the pressure in the transition region is increased above $p_0/2$ by a separate valve, causing the pressure differential across the upper stainless steel diaphragm to increase, and eventually to break. Conceptually the break is very rapid, but there appeared to be a significant lag in the measured values, when compared with the theoretical predictions as illustrated in Fig. 4. To explain this, we undertook a study of the effect of large ductility of the stainless steel diaphragms on depressurization.

The analysis is intended to characterize the rupture only in a qualitative way. A more precise analysis would not be justified since we are not really interested in slow rupture, and stress-strain data for the stainless steel shim stock used is not readily available.

It is assumed that the stress-strain relationship has the form

$$\sigma = \sigma_0 + \sigma_u (\varepsilon/\varepsilon_u)^{\frac{1}{2}}$$

where σ_0 is the yield stress, σ_u is the ultimate strength and ε_u is the strain at failure. To compute the strain we assume that the diaphragm assumes the shape of a spherical segment with radius R. Taking r as the radius of the pipe and δ as the deflection of the diaphragm, we find

$$\sin \theta = \frac{2r\delta}{\delta^2 + r^2}$$

where θ is the angle between the pipe axis and the normal to the diaphragm at its junction with the pipe. Then the strain is given by

$$\varepsilon = \theta \frac{\delta^2 + r^2}{2\delta r} - 1.$$

In the course of the rupture process the rate of deflection and fluid velocity in the pipe, u , are related by

$$\dot{\delta} = \frac{2r^2}{r^2 + \delta^2} u.$$

Finally, the pressure adjacent to the diaphragm can be obtained from the equilibrium condition

$$p = \frac{4h\delta}{r^2 + \delta^2} \sigma.$$

These formulas, together, provide a boundary condition relating pressure and velocity at the end of the pipe, and can be readily introduced into the SOLA-FLX program.

The initial value for δ can be determined explicitly when the small angle formula for $\sin^{-1}\theta$ is used, leading to

$$\varepsilon = 2\delta_0^2/3r^2$$

where δ_0 denotes the initial value of diaphragm deflection and ε_0 is the initial strain. By combining this with the other relations obtained above and defining

$$x = \sqrt{\varepsilon/\varepsilon_u}$$

we find the initial strain is given by

$$x = (a/q + 1/4q^2)^{\frac{1}{2}} - 1/2q$$

where

$$a = \Delta p_0 r / \sigma_u h \sqrt{24 \epsilon_u}$$

and

$$q = \sigma_u / \sigma_0 .$$

The pressure history at P5 obtained using this description of diaphragm bursting is compared with the experimental data in Fig. 5. The initial test pressure is probably higher than the prescribed test pressure of 152 bars because of inaccuracies in the mechanical gauge used to set the initial pressure. Results for other gauges are shown in Figs. 6, 7 and 8. Since the data for the various gauges come from several tests with varying initial pressures, it did not appear reasonable to rerun the calculations. In any case, these tests were only intended to be exploratory in character. We believe that they do show that calculations and experiments can be made to agree fairly well in a simple geometry. A comparison of measured and computed hoop stresses 2.7 cm below the top of the CSB is shown in Fig. 9 for an instantaneous break and in Fig. 10 using the diaphragm treatment. It is clear that the diaphragm treatment, though approximate, significantly improves the agreement.

One test with a side port break and a double diaphragm was also run, and showed evidence of plastic deformation of the CSB. The apparatus could be used for a variety of parameter studies, though no further tests are planned.

3. Comparison of Two- and Three-Dimensional Calculations

In the SOLA-FLX code we have made the assumption that circumferential and axial motions dominate the flow in the downcomer of a PWR following a LOCA. The geometry is illustrated in Fig. 11, which is taken from Ref. 10 and compares a typical PWR and the HDR geometry. At early times, when the rarefaction front is confined to the downcomer, the assumption of fluid motion tangential to the downcomer is clearly plausible. At late times, however, the motion in the lower plenum and core regions is strongly three-dimensional. To investigate the importance of these three-dimensional effects we compared calculations with the two-dimensional SOLA-FLX code [15] and the three-dimensional K-FIX(3D-FLX) code [16]. The calculation simulates the loss of coolant experiments planned for the HDR test facility and described by Krieg et al. [10]. In these calculations we have, however, omitted the mass ring at the bottom of the CSB. We have found that it is necessary in SOLA-FLX to represent the depressurization in the lower plenum and core to make the calculations realistic out to 40 ms. For this purpose we set the pressure in the lower plenum and core to

$$\bar{p} = p_0 - c^2 \delta m / V$$

where δm is the mass loss from the lower plenum into the downcomer, c is an average sound speed and V is the volume of the three-dimensional region. The radial deflection of the downcomer in the plane containing the break is shown at 10, 20, 30 and 40 ms in Fig. 12 in which the coupled and uncoupled calculations are compared. It is curious that the deflection at the bottom of the cylinder is opposite to the flow out the cold leg. A careful examination of the computer output data shows that this is caused by the complexity of the coupling. Specifically, a wave propagates down the steel CSB faster than in the fluid-filled

downcomer, and the motion of the CSB is outward, as a result of the transient pressure drop. The outward motion causes compression of the fluid adjacent to the wave in the downcomer. Above the bump the fluid moves upward and below the bump it moves downward. This precursor in the fluid forces the CSB to move inward before the outward moving wave arrives. In Fig. 13 the results of the two and three dimensional calculations are compared. We believe that the similarity of the two calculations is due to the dominating effect of the virtual mass of the fluid in the downcomer region, which is given by

$$M_d^v = (r/b)^2 M_d$$

Here M_d denotes the mass of the downcomer fluid in any section, r and b denote the radius and gap of the downcomer and M_d^v represents the virtual mass of the fluid in any section. This result is a special case of the general analysis of Brennen [18]. The very large value of the ratio r/b for PWRs causes the virtual mass to dominate the inertial effects in these calculations, and hence the motion of the fluid in the core region is of secondary importance, though not negligible.

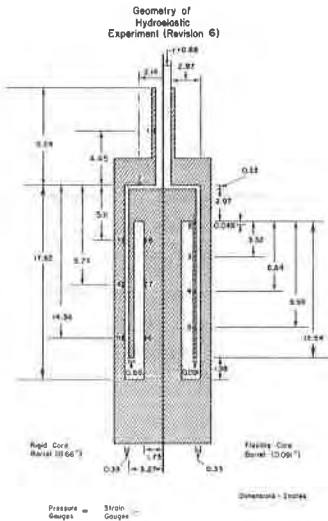


Fig. 1. Cross section of S^3 test apparatus.

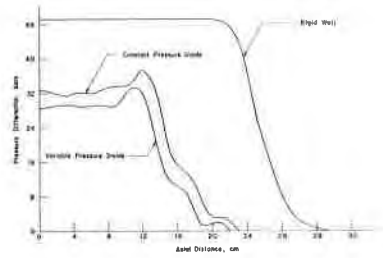


Fig. 2. Comparison of coupled and uncoupled wave propagation problems in axisymmetric geometry.

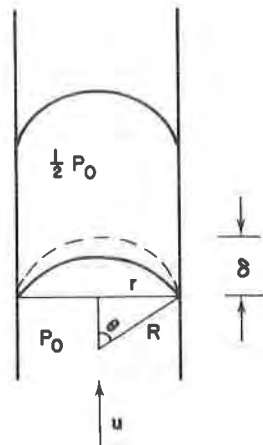


Fig. 3. Idealization of double-diaphragm used in S^3 test apparatus.

Comparison of Computed and Measured Pressure P5a

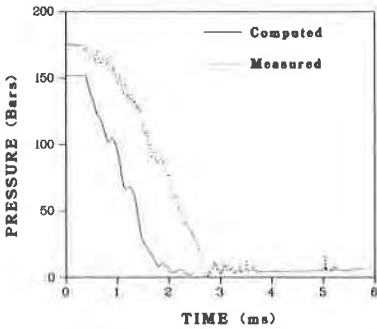


Fig. 4. Comparison of computed and measured pressure histories at P5, assuming instantaneous pressure release.

Comparison of Computed and Measured Pressure P5

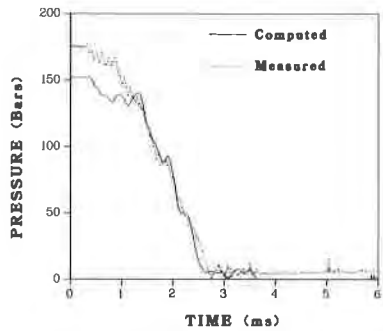


Fig. 5. Comparison of computed and measured pressure histories at P5 with double-diaphragm model.

Comparison of Computed and Measured Pressure P1

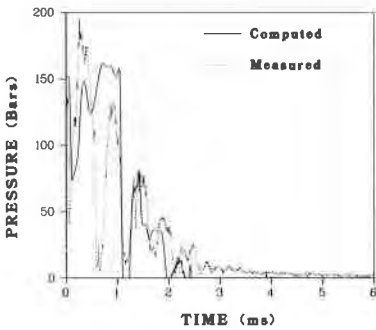


Fig. 6. Comparison of computed and measured pressure histories at P1 with double-diaphragm model.

Comparison of Computed and Measured Pressure P3

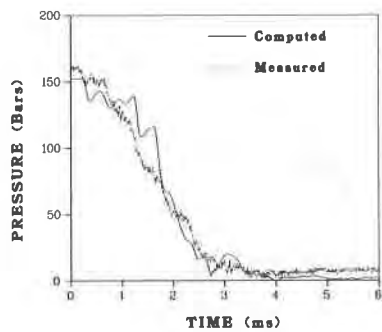


Fig. 7. Comparison of computed and measured pressure histories at P3 with double-diaphragm model.

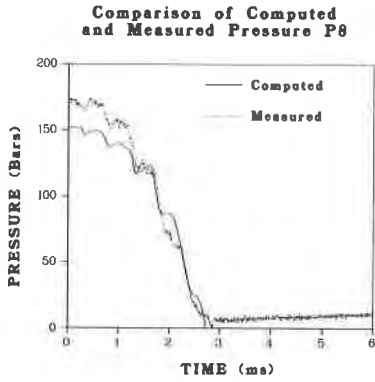


Fig. 8. Comparison of computed and measured pressure histories at P8 with double-diaphragm model.

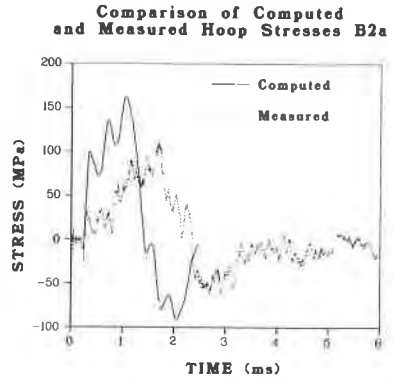


Fig. 9. Comparison of computed and measured hoop stress 2.7 cm below the top of the CSB with instantaneous pressure release.

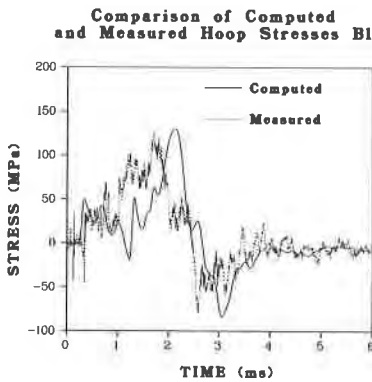


Fig. 10. Comparison of computed and measured hoop stress 2.7 cm below the top of the CSB with double-diaphragm model.

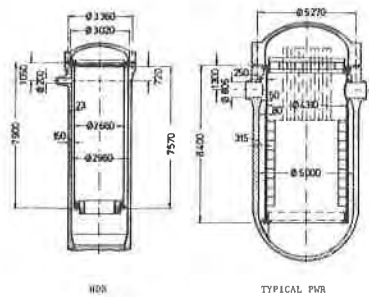


Fig. 11. Comparison of a typical PWR with HDR test reactor.

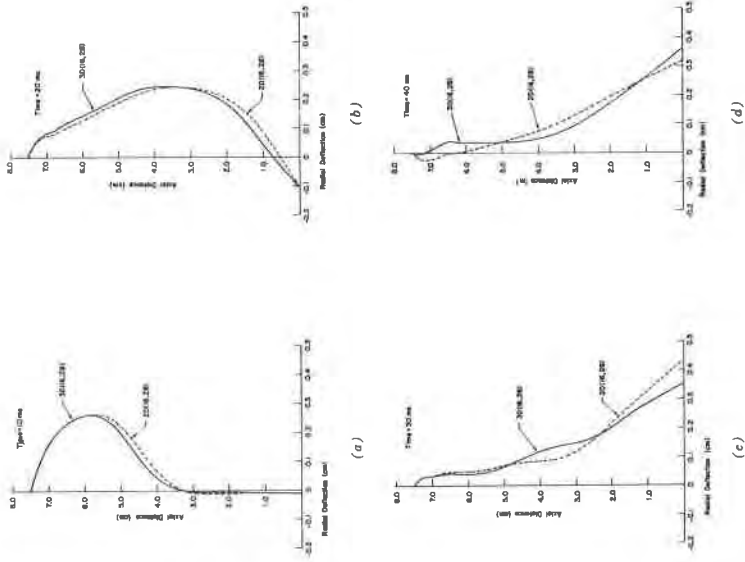


Fig. 12. Comparison of radial deflection profile of the CSB in a plane containing the break, with and without coupling, at 4 times.

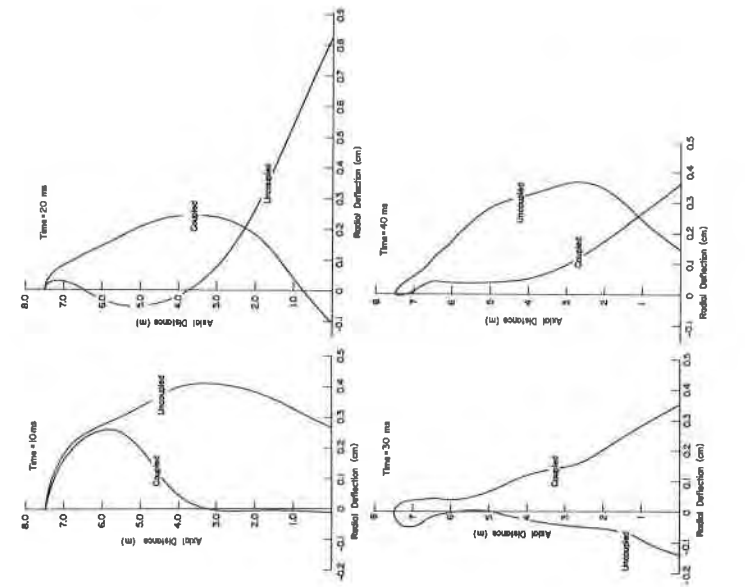


Fig. 13. Comparison of radial deflection profile of the CSB in a plane containing the break as computed using two-dimensional and three-dimensional coupled codes.

References

- [1] BELYTSCHKO, T., "Computational Methods for Fluid/Structure Interaction in Reactor Safety Analysis," Trans. 4th Int'l Conf. on Structural Mechanics in Reactor Technology, San Francisco, Aug. 1977.
- [2] DONÉA, J., FOSOLI-STELLA, P., and GIULIANI, S., "Lagrangian and Eulerian Finite Element Techniques for Transient Fluid-Structure Interaction Problems," *ibid.*
- [3] DIENES, J. K., HIRT, C. W., and STEIN, L. R., "Hydro-Elastic Calculations of the Dynamic Reponse of a Reactor to a Sudden Loss of Coolant," *ibid.*
- [4] MARCAL, P. V. and WERTHEIMER, T. B., "Fluid-Solid Interaction by Finite Element Techniques," *ibid.*
- [5] GROSS, M. B. and HOFFMAN, R., "Fluid-Structure Interaction Calculations," *ibid.*
- [6] NAHAVANDI, A. N., PEDRIDO, R. R. and CLOUD, R. L., "Dynamic Analysis of Structures with Solid-Fluid Interaction," *ibid.*
- [7] YOUNGDAHL, C. K. and KOT, C. A., "PTA-1 Computer Program for Treating Pressure Transients in Hydraulic Networks Including the Effect of Pipe Plasticity," *ibid.*
- [8] HUBER, A. and HOFFMAN, H., "Coupled Structure-Fluid Analysis for a PWR Burst Protection Design," *ibid.*
- [9] DUBOIS, J. J. and DE ROUVRAY, "Improved Coupled Euler-Lagrange Finite Element Analysis of the Fluid-Structure Dynamic Interaction Problem," *ibid.*
- [10] KRIEG, R., SCHLECHTENDAHL, E. G., SCHOLL, K.-H. and SCHUMANN, U., "Full-Scale HDR Blowdown Experiments as a Tool for Investigating Dynamic Fluid-Structural Coupling," *ibid.*
- [11] KATZ, F., KRIEG, R., LUDWIG, A., SCHLECHTENDAHL, E. G. and STÖLTING, K., "2D Fluid Flow in the Downcomer and Dynamic Response of the Core Barrel during PWR Blowdown," *ibid.*
- [12] DIENES, J. K., HIRT, C. W. and STEIN, L. R., "Multi-dimensional Fluid-Structure Interactions in a Pressurized Water Reactor," Computational Methods for Fluid-Structure Interaction Problems, Proceedings of the Winter Annual Meeting of the American Society of Mechanical Engineers, Atlanta, Georgia, December, 1978, appearing in publication AMD 26 of the ASME.
- [13] TIMOSHENKO, S., Theory of Plates and Shells, McGraw-Hill, 1940.
- [14] HIRT, C. W. and ROMERO, N. C., "Applications of a Drift-Flux Model to Flashing in Straight Pipes," Los Alamos Scientific Laboratory report LA-6005, July, 1965.
- [15] DIENES, J. K., HIRT, C. W. and STEIN, L. R., "Computer Simulation of the Hydroelastic Response of a Pressurized Water Reactor to a Sudden Depressurization," Los Alamos Scientific Laboratory report LA-NUREG-6772-MS, April, 1977.
- [16] RIVARD, W. C. and TORREY, M. D., "Fluid-Structure Response of a Pressurized Water Reactor Core Barrel during Blowdown," Los Alamos Scientific Laboratory Report LA-7404, July, 1978.
- [17] RIVARD, W. C. and TORREY, M. D., "K-FIX: A Computer Program for Transient, Two-Dimensional, Two-Fluid Flow," Los Alamos Scientific Laboratory report LA-NUREG-6623, April, 1977.
- [18] BRENNEN, C., "On the Flow in an Annulus Surrounding a Whirling Cylinder," *J. Fluid Mech.*, 75, 1976.